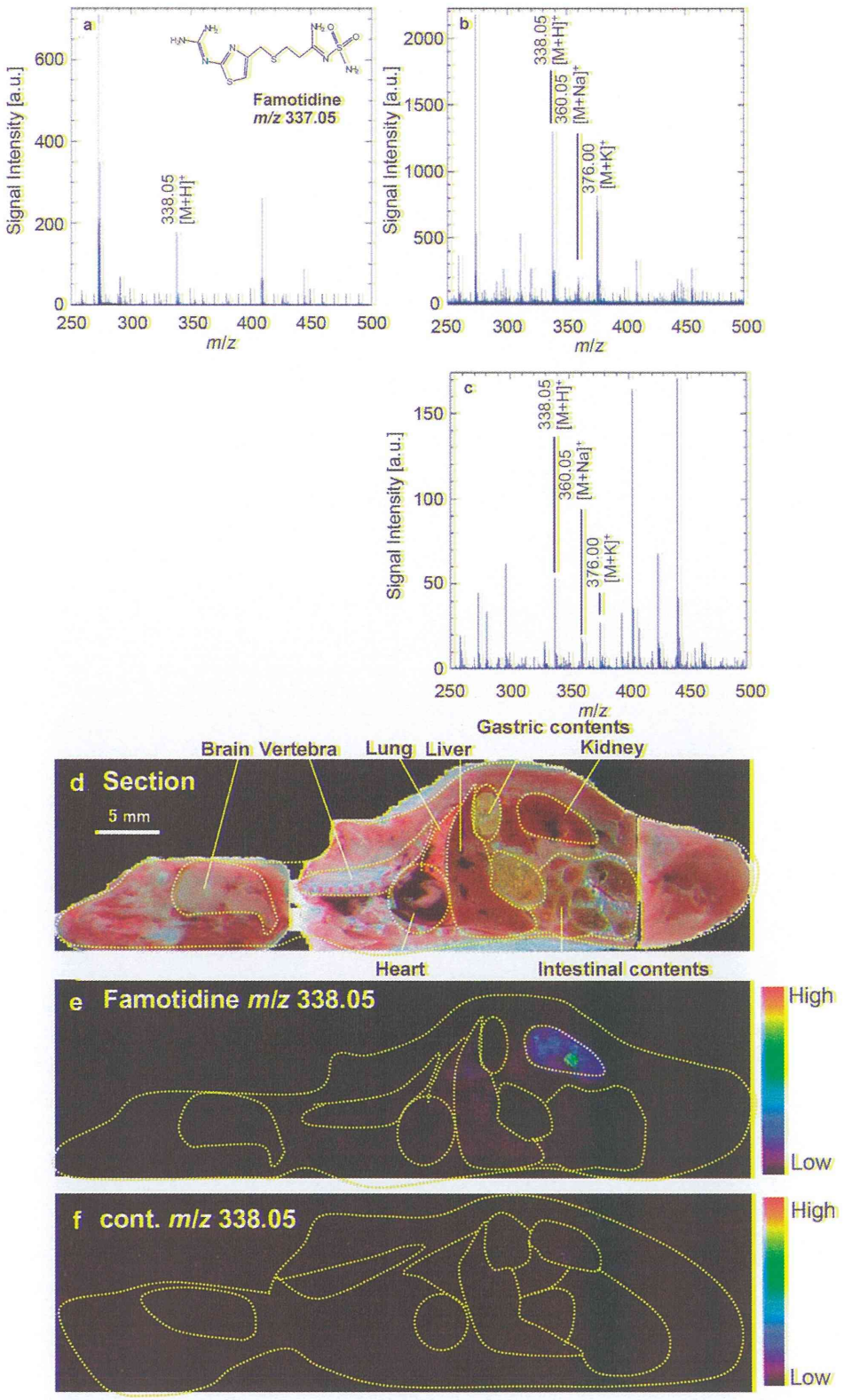


Fig. 5. Mass Spectrum of Famotidine and an MS Ion Image of a Whole-Body Section

(A) Structure and mass spectrum of famotidine. (B) Mass spectrum of famotidine detected in a tissue section. (C) Mass spectrum of famotidine detected in the kidney in a tissue section. (D) Optical image of a mouse tissue section. (E) MS ion image of famotidine (*m/z* 338.05) on a mouse tissue section 3 min after injection. Famotidine is localized to a significant extent in the kidney. (F) MS ion image at *m/z* 338.05 on a control mouse tissue section. (Reprinted from ref. 69 with permission from Journal of the Mass Spectrometry Society of Japan.)

applied this system to analyze human hair cross sections, and have detected biomolecules showing aging-related alterations. The optical images obtained at high resolution showed molecular distribution in the cortex and medulla region of hair.[68] Among the 31 molecules detected specifically in hair sections, dihydrouracil and 3,4-dihydroxymandelic acid (DHMA), which are metabolites of uracil and catecholamines, respectively, exhibited a higher signal intensity in the young group than in the old, and *O*-phosphoethanolamine displayed a higher intensity in the old group (Fig. 4). Among the 3, putative *O*-phosphoethanolamine showed a cortex-specific distribution, and exhibited changes in signal intensity with aging, whereas the molecules in medulla did not exhibit significant changes.

**3.4. Analysis of Drug Distribution** Imaging of drugs and metabolites by MALDI-IMS offers a unique opportunity to identify changes in the distribution of a desired compound in different regions of a tissue of interest, and this technique can help us to understand whether an exogenous compound administered orally affects endogenous metabolites. Antipsychotic, cancer, anti-anxiety, and hypnotic drugs have been studied in different tissue sections by IMS to determine the distribution of molecules.[43] In these assays, a multivariate approach with MALDI-IMS is useful to investigate the dynamics of metabolites.[44] Recently, we attempted to visualize the distribution of famotidine with a higher spatial resolution in whole body mouse sections using the mass microscope that we developed, and observed famotidine was mainly distributed in the kidney (Fig. 5).[69] Moreover, a higher spatial-resolution analysis revealed that the distribution of famotidine was in the renal pelvis of the kidney. The results suggest that famotidine is concentrated in the renal pelvis through the cortex and marrow in the kidney during the excretion process. It can therefore be concluded that the mass microscope permits deeper insight into therapeutic and toxicological processes associated with drug administration.

## 4. FUTURE PERSPECTIVES

Many great advances have been made in MALDI-IMS to resolve molecular species in various types of biological samples, but there is still room for improvement with respect to sample preparation, ionization, and instrumentation. The mass microscope could be a powerful tool for obtaining high resolution of biomolecules in tissue samples. The fundamental contributions of MALDI-IMS will provide a powerful tool for the early detection and characterization of cellular processes in both healthy and disease conditions, and help us to understand and treat disorders very effectively.

**Acknowledgments** This review was undertaken on behalf of The Pharmaceutical Society of Japan for Awarding the Promotion Prize to M.S. for the development and application of IMS techniques and mass microscope. We would like to acknowledge the collaboration of past and present colleagues in the Department of Cell Biology and Anatomy of Hamamatsu University School of Medicine, Shimadzu Corporation, and many other collaborators for their work that was reviewed in this paper and supported mainly by the Japanese Science and Technology Agency (JST) in the form of a Grant-in-Aid for SENTAN.

## REFERENCES

1) Kevles B. *Naked to the Bone: Medical Imaging in the Twentieth Century*. Rutgers University Press, New Brunswick, New Jersey, 1997.
2) Weissleder R, Moore A, Mahmood U, Bhorade R, Benveniste H, Chiocca EA, Basilion JP. *In vivo* magnetic resonance imaging of transgene expression. *Nat. Med.*, **6**, 351–355 (2000).
3) Setou M, Radostin D, Atsuzawa K, Yao I, Fukuda Y, Usuda N, Nagayama K. Mammalian cell nano structures visualized by cryo Hilbert differential contrast transmission electron microscopy. *Med. Mol. Morphol.*, **39**, 176–180 (2006).
4) Phelps ME, Hoffman EJ, Mullani NA, Ter-Pogossian MM. Application of annihilation coincidence detection to transaxial reconstruction tomography. *Journal of Nuclear Medicine*, **16**, 210–224 (1975).
5) Ikegami K, Heier RL, Taruishi M, Takagi H, Mukai M, Shimma S, Taira S, Hatanaka K, Morone N, Yao I, Campbell PK, Yuasa S, Janke C, Macgregor GR, Setou M. Loss of alpha-tubulin polyglutamylation in ROSA22 mice is associated with abnormal targeting of KIF1A and modulated synaptic function. *Proc. Natl. Acad. Sci. U.S.A.*, **104**, 3213–3218 (2007).
6) Yao I, Takagi H, Ageta H, Kahyo T, Sato S, Hatanaka K, Fukuda Y, Chiba T, Morone N, Yuasa S, Inokuchi K, Ohtsuka T, Macgregor GR, Tanaka K, Setou M. SCRAPPER-dependent ubiquitination of active zone protein RIM1 regulates synaptic vesicle release. *Cell*, **130**, 943–957 (2007).
7) Hatanaka T, Hatanaka Y, Setou M. Regulation of amino acid transporter ATA2 by ubiquitin ligase Nedd4-2. *J. Biol. Chem.*, **281**, 35922–35930 (2006).
8) Ikegami K, Mukai M, Tsuchida J, Heier RL, Macgregor GR, Setou M. TTLL7 is a mammalian beta-tubulin polyglutamylase required for growth of MAP2-positive neurites. *J. Biol. Chem.*, **281**, 30707–30716 (2006).
9) Hatanaka T, Hatanaka Y, Tsuchida J-i, Ganapathy V, Setou M. Amino acid transporter ATA2 is stored at the *trans*-Golgi network and released by insulin stimulus in adipocytes. *J. Biol. Chem.*, **281**, 39273–39284 (2006).
10) Konishi Y, Setou M. Tubulin tyrosination navigates the kinesin-1 motor domain to axons. *Nat. Neurosci.*, **12**, 559–567 (2009).
11) Yang HJ, Takagi H, Konishi Y, Ageta H, Ikegami K, Yao I, Sato S, Hatanaka K, Inokuchi K, Seog DH, Setou M. Transmembrane and ubiquitin-like domain-containing protein 1 (Tmub1/HOPS) facilitates surface expression of GluR2-containing AMPA receptors. *PLoS ONE*, **3**, 1–13 (2008).
12) Fukuda Y, Kawano Y, Tanikawa Y, Oba M, Koyama M, Takagi H, Matsumoto M, Nagayama K, Setou M. *In vivo* imaging of the dendritic arbors of layer V pyramidal cells in the cerebral cortex using a laser scanning microscope with a stick-type objective lens. *Neurosci. Lett.*, **400**, 53–57 (2006).
13) Asai S, Takamura K, Suzuki H, Setou M. Single-cell imaging of c-fos expression in rat primary hippocampal cells using a luminescence microscope. *Neurosci. Lett.*, **434**, 289–292 (2008).
14) Setou M, Seog D-H, Tanaka Y, Kanai Y, Takei Y, Kawagishi M, Hirokawa N. Glutamate-receptor-interacting protein GRIP1 directly steers kinesin to dendrites. *Nature*, **417**, 83–87 (2002).
15) Luxembourg SL, Mize TH, McDonnell LA, Heeren RMA. High-spatial resolution mass spectrometric imaging of peptide and protein distributions on a surface. *Anal. Chem.*, **76**, 5339–5344 (2004).
16) Brotherton HO, Yost RA. Determination of drugs in blood serum by mass spectrometry/mass spectrometry. *Anal. Chem.*, **55**, 549–553 (1983).
17) Johnson JV, Yost RA, Faull KF. Tandem mass spectrometry for the trace determination of tryptolines in crude brain extracts. *Anal. Chem.*, **56**, 1655–1661 (1984).
18) Bernier UR, Kline DL, Barnard DR, Schreck CE, Yost RA.

Analysis of human skin emanations by gas chromatography/mass spectrometry. 2. Identification of volatile compounds that are candidate attractants for the yellow fever mosquito (*Aedes aegypti*). *Anal. Chem.*, **72**, 747–756 (2000).
19) Garrett TJ, Yost RA. Analysis of intact tissue by intermediate-pressure MALDI on a linear ion trap mass spectrometer. *Anal. Chem.*, **78**, 2465–2469 (2006).
20) Rubakhin SS, Greenough WT, Sweedler JV. Spatial profiling with MALDI MS: distribution of neuropeptides within single neurons. *Anal. Chem.*, **75**, 5374–5380 (2003).
21) Rubakhin SS, Churchill JD, Greenough WT, Sweedler JV. Profiling signaling peptides in single mammalian cells using mass spectrometry. *Anal. Chem.*, **78**, 7267–7272 (2006).
22) Miao H, Rubakhin SS, Sweedler JV. Subcellular analysis of D-aspartate. *Anal. Chem.*, **77**, 7190–7194 (2005).
23) Hatcher NG, Richmond TA, Rubakhin SS, Sweedler JV. Monitoring activity-dependent peptide release from the CNS using single-bead solid-phase extraction and MALDI TOF MS detection. *Anal. Chem.*, **77**, 1580–1587 (2005).
24) Sugiura Y, Shimma S, Setou M. Two-step matrix application technique to improve ionization efficiency for matrix-assisted laser desorption/ionization in imaging mass spectrometry. *Anal. Chem.*, **78**, 8227–8235 (2006).
25) Shimma S, Furuta M, Ichimura K, Yoshida Y, Setou M. A novel approach to *in situ* proteome analysis using chemical inkjet printing technology and MALDI-QIT-TOF tandem mass spectrometer. *Journal of the Mass Spectrometry Society of Japan*, **54**, 133–140 (2006).
26) Shimma S, Furuta M, Ichimura K, Yoshida Y, Setou M. Direct MS/MS analysis in mammalian tissue sections using MALDI-QIT-TOF-MS and chemical inkjet technology. *Surf. Interface Anal.*, **38**, 12–13, 1712–1714 (2006).
27) Chaurand P, Schwartz SA, Reyzer ML, Caprioli RM. Imaging mass spectrometry: principles and potentials. *Toxicol. Pathol.*, **33**, 92–101 (2005).
28) Stoeckli M, Chaurand P, Hallahan DE, Caprioli RM. Imaging mass spectrometry: a new technology for the analysis of protein expression in mammalian tissues. *Nat. Med.*, **7**, 493–496 (2001).
29) Sugiura Y, Shimma S, Moriyama Y, Setou M. Direct analysis of cultured cells with matrix-assisted laser desorption/ionization on conductive transparent film. *Journal of the Mass Spectrometry Society of Japan*, **55**, 25–31 (2007).
30) Chaurand P, Schriver KE, Caprioli RM. Instrument design and characterization for high resolution MALDI-MS imaging of tissue sections. *J. Mass Spectrom.*, **42**, 476–489 (2007).
31) Schwartz SA, Weil RJ, Johnson MD, Toms SA, Caprioli RM. Protein profiling in brain tumors using mass spectrometry: feasibility of a new technique for the analysis of protein expression. *Clin. Cancer Res.*, **10**, 981–987 (2004).
32) Pierson J, Norris JL, Aerni HR, Svenningsson P, Caprioli RM, Andrén PE. Molecular profiling of experimental Parkinson's disease: direct analysis of peptides and proteins on brain tissue sections by MALDI mass spectrometry. *J. Proteome Res.*, **3**, 289–295 (2004).
33) Jackson SN, Wang H-YJ, Woods AS. *In situ* structural characterization of phosphatidylcholines in brain tissue using MALDI-MS/MS. *J. Am. Soc. Mass Spectrom.*, **16**, 2052–2056 (2005).
34) Jackson SN, Wang H-YJ, Woods AS, Ugarov M, Egan T, Schultz JA. Direct tissue analysis of phospholipids in rat brain using MALDI-TOFMS and MALDI-ion mobility-TOFMS. *J. Am. Soc. Mass Spectrom.*, **16**, 133–138 (2005).
35) Touboul D, Piednoël H, Voisin V, De La Porte S, Brunelle A, Halgand F, Laprévote O. Changes of phospholipid composition within the dystrophic muscle by matrix-assisted laser desorption/ionization mass spectrometry and mass spectrometry imaging. *Eur. J. Mass Spectrom.* (Chichester, Eng.), **10**, 657–664 (2004).
36) Khatib-Shahidi S, Andersson M, Herman JL, Gillespie TA, Caprioli RM. Direct molecular analysis of whole-body animal tissue sections by imaging MALDI mass spectrometry. *Anal. Chem.*, **78**, 6448–6456 (2006).
37) Takáts Z, Wiseman JM, Gologan B, Cooks RG. Mass spectrometry sampling under ambient conditions with desorption electrospray ionization. *Science*, **306**, 471–473 (2004).
38) Benninghoven A. Surface investigation of solids by the statical method of secondary ion mass spectroscopy (SIMS). *Surf. Sci.*, **35**, 427–457 (1973).
39) Tanaka K, Waki H, Ido Y, Akita S, Yoshida Y, Yoshida T, Matsuo T. Protein and polymer analyses up to *m/z* 100000 by laser ionization time-of-flight mass spectrometry. *Rapid Commun. Mass Spectrom.*, **2**, 151–153 (1988).
40) Rohner TC, Staab D, Stoeckli M. MALDI mass spectrometric imaging of biological tissue sections. *Mech. Ageing Dev.*, **126**, 177–185 (2005).
41) Shimma S, Sugiura Y, Hayasaka T, Zaima N, Matsumoto M, Setou M. Mass imaging and identification of biomolecules with MALDI-QIT-TOF-based system. *Anal. Chem.*, **80**, 878–885 (2008).
42) Sugiura Y, Konishi Y, Zaima N, Kajihara S, Nakanishi H, Taguchi R, Setou M. Visualization of the cell-selective distribution of PUFA-containing phosphatidylcholines in mouse brain by imaging mass spectrometry. *J. Lipid Res.*, **50**, 1776–1788 (2009).
43) Sugiura Y, Shimma S, Konishi Y, Yamada MK, Setou M. Imaging mass spectrometry technology and application on ganglioside study; visualization of age-dependent accumulation of C20-ganglioside molecular species in the mouse hippocampus. *PLoS ONE*, **3**, 1–9 (2008).
44) Zaima N, Matsuyama Y, Setou M. Principal component analysis of direct matrix-assisted laser desorption/ionization mass spectrometric data related to metabolites of fatty liver. *J. Oleo Sci.*, **58**, 267–273 (2009).
45) Goto-Inoue N, Hayasaka T, Zaima N, Setou M. The specific localization of seminolipid molecular species on mouse testis during testicular maturation revealed by imaging mass spectrometry. *Glycobiology*, **19**, 950–957 (2009).
46) Hayasaka T, Goto-Inoue N, Sugiura Y, Zaima N, Nakanishi H, Ohishi K, Nakanishi S, Naito T, Taguchi R, Setou M. Matrix-assisted laser desorption/ionization quadrupole ion trap time-of-flight (MALDI-QIT-TOF)-based imaging mass spectrometry reveals a layered distribution of phospholipid molecular species in the mouse retina. *Rapid Commun. Mass Spectrom.*, **22**, 3415–3426 (2008).
47) Shimma S, Sugiura Y, Hayasaka T, Hoshikawa Y, Noda T, Setou M. MALDI-based imaging mass spectrometry revealed abnormal distribution of phospholipids in colon cancer liver metastasis. *J. Chromatogr. B Analyt. Technol. Biomed. Life Sci.*, **855**, 98–103 (2007).
48) Hosokawa N, Sugiura Y, Setou M. Spectrum Normalization Method Using an External Standard in Mass Spectrometric Imaging. *Journal of the Mass Spectrometry Society of Japan*, **56**, 77–81 (2008).
49) Goto-Inoue N, Hayasaka T, Sugiura Y, Taki T, Li YT, Matsumoto M, Setou M. High-sensitivity analysis of glycosphingolipids by matrix-assisted laser desorption/ionization quadrupole ion trap time-of-flight imaging mass spectrometry on transfer membranes. *J. Chromatogr. B*, **870**, 74–83 (2008).
50) Sugiura Y, Shimma S, Setou M. Thin sectioning improves the peak intensity and signal-to-noise ratio in direct tissue mass spectrometry. *Journal of the Mass Spectrometry Society of Japan*, **54**, 45–48 (2006).
51) Taira S, Sugiura Y, Moritake S, Shimma S, Ichiyanagi Y, Setou M. Nanoparticle-assisted laser desorption/ionization based mass imaging with cellular resolution. *Anal. Chem.*, **80**, 4761–4766 (2008).
52) Moritake S, Taira S, Sugiura Y, Setou M, Ichiyanagi Y. Magnetic nanoparticle-based mass spectrometry for the detection of biomolecules in cultured cells. *J. Nanosci. Nanotechnol.*, **9**, 169–176 (2009).
53) Ageta H, Asai S, Sugiura Y, Goto-Inoue N, Zaima N, Setou M. Layer-specific sulfatide localization in rat hippocampus middle molecular layer is revealed by nanoparticle-assisted laser desorption/

ionization imaging mass spectrometry. *Med. Mol. Morphol.*, **42**, 16–23 (2009).
54) Nakagawa T, Setou M, Seog D, Ogasawara K, Dohmae N, Takio K, Hirokawa N. A novel motor, KIF13A, transports mannose-6-phosphate receptor to plasma membrane through direct interaction with AP-1 complex. *Cell*, **103**, 569–581 (2000).
55) Setou M, Nakagawa T, Seog D-H, Hirokawa N. Kinesin superfamily motor protein KIF17 and mLin-10 in NMDA receptor-containing vesicle transport. *Science*, **288**, 1796–1802 (2000).
56) Müthing J. High-resolution thin-layer chromatography of gangliosides. *J. Chromatogr. A*, **720**, 3–25 (1996).
57) van Echten-Deckert G. Sphingolipid extraction and analysis by thin-layer chromatography. *Methods Enzymol.*, **312**, 64–79 (2000).
58) Yu RK, Ariga T. Ganglioside analysis by high-performance thin-layer chromatography. *Methods Enzymol.*, **312**, 115–134 (2000).
59) Hayasaka T, Goto-Inoue N, Zaima N, Kimura Y, Setou M. Organ-specific distributions of lysophosphatidylcholine and triacylglycerol in mouse embryo. *Lipids*, **44**, 837–848 (2009).
60) Valdes-Gonzalez T, Goto-Inoue N, Hirano W, Ishiyama H, Hayasaka T, Setou M, Taki T. New approach for glyco- and lipidomics—molecular scanning of human brain gangliosides by TLC-Blot and MALDI-QIT-TOF MS. *J. Neurochem.*, **116**, 678–683 (2011).
61) Ikegami K, Horigome D, Mukai M, Livnat I, MacGregor GR, Setou M. TTLL10 is a protein polyglycylase that can modify nucleosome assembly protein 1. *FEBS Lett.*, **582**, 1129–1134 (2008).
62) Hatanaka K, Ikegami K, Takagi H, Setou M. Hypo-osmotic shock induces nuclear export and proteasome-dependent decrease of UBL5. *Biochem. Biophys. Res. Commun.*, **350**, 610–615 (2006).
63) Morita Y, Ikegami K, Goto-Inoue N, Hayasaka T, Zaima N, Tanaka H, Uehara T, Setoguchi T, Sakaguchi T, Igarashi H, Sugimura H, Setou M, Konno H. Imaging mass spectrometry of gastric carcinoma in formalin-fixed paraffin-embedded tissue microarray. *Cancer Sci.*, **101**, 267–273 (2010).
64) Yao I, Sugiura Y, Matsumoto M, Setou M. *In situ* proteomics with imaging mass spectrometry and principal component analysis in the Scrapper-knockout mouse brain. *Proteomics*, **8**, 3692–3701 (2008).
65) Setou M, Hayasaka T, Shimma S, Sugiura Y, Matsumoto M. Protein denaturation improves enzymatic digestion efficiency for direct tissue analysis using mass spectrometry. *Appl. Surf. Sci.*, **255**, 1555–1559 (2008).
66) Harada T, Yuba-Kubo A, Sugiura Y, Zaima N, Hayasaka T, Goto-Inoue N, Wakui M, Suematsu M, Takeshita K, Ogawa K, Yoshida Y, Setou M. Visualization of volatile substances in different organelles with an atmospheric-pressure mass microscope. *Anal. Chem.*, **81**, 9153–9157 (2009).
67) Onoue K, Zaima N, Sugiura Y, Isojima T, Okayama S, Horii M, Akai Y, Uemura S, Takemura G, Sakuraba H, Sakaguchi Y, Setou M, Saito Y. Using imaging mass spectrometry to accurately diagnose Fabry's disease. *Circ. J.*, **75**, 221–223 (2011).
68) Waki ML, Onoue K, Takahashi T, Goto K, Saito Y, Inami K, Makita I, Angata Y, Suzuki T, Yamashita M, Sato N, Nakamura S, Yuki D, Sugiura Y, Zaima N, Goto-Inoue N, Hayasaka T, Shimomura Y, Setou M. Investigation by imaging mass spectrometry of biomarker candidates for aging in the hair cortex. *PLoS ONE*, **6**, 1–9 (2011).
69) Saito Y, Hayasaka T, Onoue K, Takizawa Y, Kajihara S, Ogawa K, Setou M. Pharmacokinetic analysis using a high spatial-resolution mass microscope. *Journal of the Mass Spectrometry Society of Japan*, **59**, 79–84 (2011).

DOI: 10.1002/cbic.201200146

# High-Resolution Multi-isotope Imaging Mass Spectrometry Enables Visualisation of Stem Cell Division and Metabolism

Kensuke Goto, Michihiko Waki, Tsukasa Takahashi, Makoto Kadowaki, and Mitsutoshi Setou*[a]

The "immortal-strand hypothesis" predicts the random segregation of chromosomes during asymmetric stem-cell division. Stem cells exhibit two cell division patterns, namely symmetric and asymmetric division. When a stem cell divides asymmetrically into two cells, it produces two different kinds of cells, namely a daughter cell that will remain a stem cell and a progenitor cell with limited self-renewal potential. During asymmetric division, the stem cell synthesises new DNA strands from the old DNA template. In this hypothesis, the parental stem cell distributes the old and new strands to the daughter and progenitor cells, respectively, so that the stem cell retains the old strand through every asymmetric division. It was proposed by John Cairns in 1975 that it is preferable for old DNA strands to be retained in parental stem cells in order to avoid any accumulation of mutations in their genome.[1]

The validity of this hypothesis has been extensively argued over a long period of time. Primary studies have examined the hypothesis in simple organisms showing asymmetric cell division, such as bacteria, plants, and fungi. An initial report on budding yeast showed, by using autoradiography, asymmetric strand segregation between parent and daughter cells.[2] This result was, however, not confirmed in subsequent fluorescence analysis of bromodeoxyuridine (BrdU) incorporation, although it must be borne in mind that different strains were used.[3] Regarding the in vivo assessment of stem cells in mammalian tissues, Potten and colleagues first reported positive evidence in a stem cell population of mouse small-intestinal epithelium.[4] This assessment involved the use of DNA synthesis markers: $^{3}$H-thymidine to label the oldest strands, and BrdU, to label newly synthesised strands. As shown by the authors, cells carrying both $^{3}$H-thymidine and BrdU were observed in the stem-cell region soon after the administration of BrdU, whereas BrdU labelling was rapidly cleared from those cells that continued to retain $^{3}$H-thymidine over the next several days: this resulted in these stem cells being called label-retaining cells or LRCs. This and subsequent studies using a similar approach have been considered to provide highly supportive evidence of nonrandom template-strand segregation; LRCs in the mouse mammary gland were shown to divide while retaining their old template DNA strands labelled with $^{3}$H-thymidine.[5] Adult muscle satellite cells, which possess stem-cell-like properties, were shown to have an LRC subpopulation in vivo.[6] Neural stem cells labelled with BrdU showed retention of the BrdU signal after division in vitro.[7] On the other hand, asymmetric segregation of chromosomes has not been confirmed in haematopoietic stem cells in vitro or in vivo, thus indicating that asymmetric segregation is not a general property of stem cells.[8]

In ■■a new *OK?*■■ study, the authors used the powerful technique of multi-isotope imaging mass spectrometry (MIMS) to provide evidence that chromosomes are randomly segregated into two kinds of cells during asymmetric stem cell division.[9] MIMS offers unique capabilities for isotopic measurement and imaging (down to 50 nm lateral resolution), which, combined with an isotopic (or elemental) labelling strategy, allows biologists to view and quantify turnovers and to follow the fate of biomolecules with a resolution sufficient for the observation of intracellular compartments. The technique is based essentially on secondary ion-microprobe mass spectrometry (SIMS; Figure 1 A).[10] SIMS is a classical ionisation method that utilises an ion beam as a means of sputtering molecules onto samples. The ion beam is so strong that molecules on tissues are disrupted to the level of atoms. Thus, the MIMS system uses SIMS to detect sputtered atoms according to their mass. Therefore, MIMS achieves several key features simultaneously, including high spatial resolution, high sensitivity, high mass resolution, parallel acquisition of masses (seven molecular species at most) and fast acquisition of ions. Acquired data on multiple planes are compressed to form a single mass image in order to reduce matrix effects and to increase the number of counts of secondary ions (Figure 1 B). Mass images obtained for two species of atoms are used to form a hue-saturation image, a representation of the isotope ratio within a sample (Figure 1 C). Furthermore, thanks to recent improvements, isotope ratio reproducibility of a few tenths per ■■million *OK?* ■■ can now be achieved.

The technique was first termed MIMS in 2004[11] and has been applied to cultured cells, human hair and bacteria.[12] In human hair, the elemental compositions of melanin granules and other components of the hair shaft were determined by observing naturally occurring atoms such as $^{16}$O, $^{14}$N and $^{32}$S. In addition, recent application of the technique in bacteria has

[a] *K. Goto, Dr. M. Waki, T. Takahashi, M. Kadowaki, Prof. Dr. Dr. M. Setou*
*Department of Cell Biology and Anatomy*
*Hamamatsu University, School of Medicine*
*1-20-1 Handayama, Hamamatsu, Shizuoka 431-3192 (Japan)*
*E-mail: setou@hama-med.ac.jp*

  

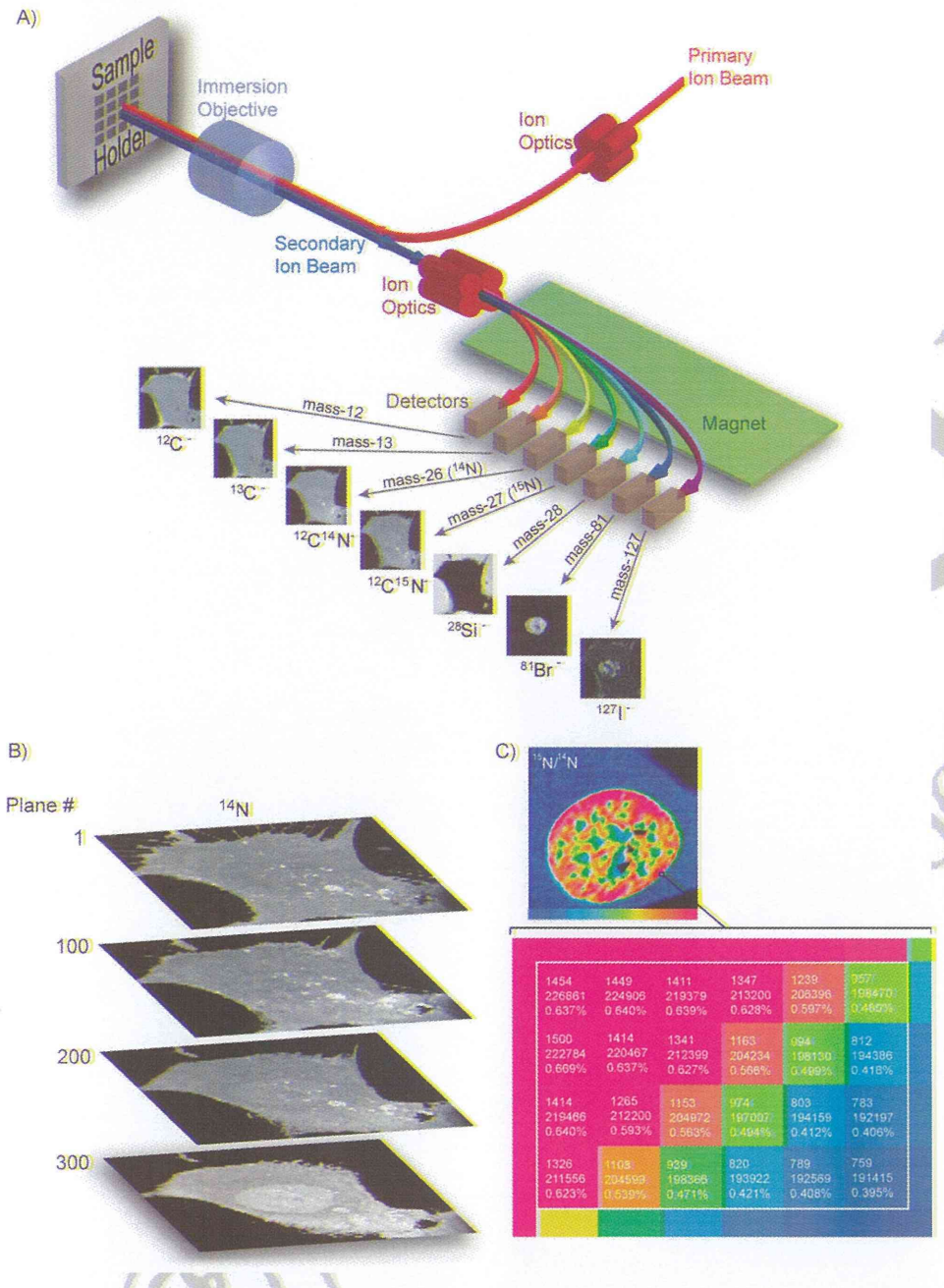


**Figure 1.** Multi-isotope imaging mass spectrometry (MIMS). A) Schematic depiction of the MIMS method. B) Ion images of successive planes acquired at the same location. Many successive planes can be compressed to form a single image so as to reduce errors. C) A quantitative ratio image—a hue-saturation image—can be obtained by comparing the quantitative data from two different masses. Reprinted by permission from Macmillan Publishers Ltd. from ref. [9], copyright: 2012.

enabled direct imaging and measurement of nitrogen fixation and metabolism.[12e,13]

The advantages of MIMS compared with conventional methods for detecting nucleic acid metabolism are as follows: 1) MIMS can detect $^{14}N$ and $^{15}N$ as the recombinant ion ■■$CN^-$ *or* CN– ?■■ to visualise nucleic acids, thus enabling simultaneous imaging of the newly synthesised DNA strand labelled with $^{15}N$ and the intact strand containing $^{14}N$. This feature enables strict evaluation of the presence/absence of daughter strands. 2) The NanoSIMS 50 can be used to localise simultaneously two isotopes of the same element, thus avoiding artefacts due to matrix effects, and allowing unmodified molecules to be studied rather than modified ones such as BrdU, the distribution of which can also be determined by this technique. Therefore it enables critical comparison of the location of $^{14}N$/$^{15}N$-labelled and BrdU-labelled chromosomes.

First, the authors confirmed that the technique they established is useful for the detection and quantification of $^{15}N$ incorporated into cells in vitro and in vivo. They supplemented a medium containing dividing fibroblasts with $^{15}N$-thymidine or ■■and?■■ injected it into the venous blood of mice by using surgically implanted osmotic minipumps. Then, they collected jejunal segments from the mice and fixed them. After fixation, the tissues were embedded, sectioned at a thickness of 0.5 μm, and mounted on silicon chips. Thus, the atoms in the small intestine of mice were visualised, and the incorporation of $^{15}N$-thymidine was quantified.

Then they used the MIMS technique to validate the immortal-strand hypothesis in the small intestine of the mouse at two different stages. They injected $^{15}N$-thymidine into mice for eight weeks after birth; this allowed developmental stem cells to incorporate $^{15}N$-thymidine into their own DNA strands. A four-week chase was performed after adding the $^{15}N$-thymidine. Finally, they labelled proliferating cells, including stem cells, with BrdU and observed the results by using MIMS. If the hypotheses were correct, stem cells would retain the labelled thymidine in their template strands through every asymmetric division. However, the results showed no $^{15}N$ signals in the area where the existence of stem cells was expected based on the anatomical relationship with Paneth cells, which can be identified by their granules. If chromosomes containing $^{15}N$-

  

thymidine were equally segregated, the signal intensity of $^{15}N$ would halve. Therefore, these data suggest that $^{15}N$-thymidine in DNA was diluted during every asymmetric division, that is, the hypothesis is incorrect.

In their next experiment, the authors injected $^{15}N$-thymidine into mice with mature stem cells. After formation, stem cells incorporate $^{15}N$-thymidine into the newly synthesised DNA strands during asymmetric division and, therefore, do not retain $^{15}N$-thymidine in their old DNA strands, as based on the hypothesis. Two weeks after the administration of $^{15}N$-thymidine, the authors labelled proliferating cells, including stem cells, with BrdU and observed the results by using MIMS. The results showed that all proliferating cells (BrdU+) exhibited $^{15}N$ signals. Thus, stem cells retain $^{15}N$-thymidine in their DNA strands. From these data obtained during the two different stages of stem cells, the authors confirmed the random segregation of chromosomes during asymmetric division.

Finally, the authors introduced the use of MIMS for *Drosophila* and human cells, and demonstrated its utility in these applications. *Drosophila* is useful for genetic analysis of the metabolism of lipids, ■■the distribution of lipids in *Drosophila* having been studied *OK?*■■ in an in vitro system.[14] In the animal ■■insect *?*■■ model, adipose accumulates in the fat body, which is a unique tissue; many studies have analysed the regulation of adipose in this tissue. It was found that many genes that function in the fat body are conserved in both humans and *Drosophila*. In order to confirm the high resolution of MIMS, the authors used *Drosophila* as an example and visualised lipid metabolism. They labelled palmitate with $^{13}C$, and observed cells in the gut and fat body of *Drosophila*. The data show a difference in the amount of $^{13}C$-palmitate incorporation between cell types in these two organs; this is consistent with the organs' functions, namely absorption and major lipid storage, respectively. The authors also observed the amount of $^{13}C$-palmitate decay in the gut, it was estimated that a high frequency of lipid turnover would be exhibited. The findings revealed that decay followed an exponential curve, with a half-time of approximately 9 h. Moreover, this study assessed, for the first time, the application of MIMS in humans. The authors administered $^{15}N$-thymidine to volunteers by intravenous infusion and observed peripheral white blood cell smears. They found no labelled white blood cells immediately after infusion; however, they found a few labelled cells after a four-week chase. The lag time is consistent with the time it takes to release the cells from the bone marrow.

The results presented in the article by Steinhauser and co-workers are quite significant because: 1) they prove that MIMS can be used for the quantitative analysis of metabolism in living mammalian bodies; 2) they provide strong evidence to negate the hypothesis of asymmetric segregation of chromosomes in stem cells in the small intestine; and 3) they confirm that MIMS following isotope labelling can be used to analyse nucleic acids in live organisms including mammals.[15] In particular, Figure 4 of the article shows the first application of isotope labelling to live humans and subsequent MIMS analysis of cells in the peripheral blood.[9]

The asymmetric segregation of chromosomes in stem cells has been examined in many locations other than the small intestine, including the muscle, breast, brain and blood. As indicated above, the different experimental methodologies used in these studies hinder any strict comparison of results or elucidation of the universal validity of the immortal-strand hypothesis. Utilising MIMS for the assessment of stem cells in these organs will provide evidence for clarifying this hypothesis. Here, the authors have utilised the highest available spatial resolution among the reported applications of MIMS to identify the intracellular localisation of incorporated substrates at the whole-chromosomal level. Further improvements in spatial resolution will enable the visualisation of molecules at a particular location and the microstructure of the chromosomes.[16] Such visualisation may reveal the site-specificity of transcription or replication on particular chromosomes. The authors have identified the subcellular features of metabolism mainly by visualising chromosomes, lipid droplets and actin filaments; this has resulted in the simultaneous publication of two papers in the same issue of *Nature*.[9,17] Based on these findings, the subcellular compartments analysed could be extended to other compartments such as the endoplasmic reticulum, Golgi body, proteasomes and mitochondria. As some of these compartments are segregated and reconstructed upon cellular division, the precise visualisation of molecular turnover at these structures might provide significant information regarding the mechanisms of division. Using multiple isotope-labelled substrates might lead to more molecule-specific analysis, as this technique would enable visualisation of molecular structures composed of different molecular units, for example, the detection of particular DNA and peptide motifs.[18] This article has revealed the molecular behaviour of whole chromosomes, and MIMS could therefore be used for molecular biology assessments focusing more specifically on particular genes or proteins. Several factors might limit the detection of targeted molecules by MIMS analysis, for instance the efficacy of the incorporation of isotope-labelled substrates, the area of targeted cells in the section, the intracellular degradation of isotope-labelled substrates and unwanted incorporation of the isotopes into molecules out of the target range for visualisation, among others. Among the numerous different cells in the organisms, the authors presumably found stem cells in the small intestine, indicating that these particular cells might escape the problems associated with the technique. It could be beneficial to identify organs and cell populations that are not subject to these problems or to reduce these factors by using an exogenous agent in future studies.

In conclusion, Steinhauser and co-workers have established a methodology for visualising the physiological metabolism of live mammalian organisms and provided evidence to negate the theory of asymmetric chromosomal division of stem cells in the mammalian small intestine by using this method. The methodology described in this work has the potential to be applied to unlimited experimental targets; thus, future reports published by these authors are expected to extend our biological insight further.

  

**Keywords:** asymmetric division · multi-isotope imaging mass spectrometry · chromosomes · stem cells · thymidine

[1] J. Cairns, *Nature* **1975**, *255*, 197–200.
[2] D. H. Williamson, D. J. Fennell in *Molecular Genetics in Yeast* (Eds.: D. von Wettstein, J. Friis, M. Kielland-Brandt, M. Stenderup), Alfred Benson Symposium, Munksgaard, Copenhagen, **1981**, pp. 89–107.
[3] M. W. Neff, D. J. Burke, *Genetics* **1991**, *127*, 463–473.
[4] a) C. S. Potten, W. J. Hume, P. Reid, J. Cairns, *Cell* **1978**, *15*, 899–906; b) C. S. Potten, G. Owen, D. Booth, *J. Cell Sci.* **2002**, *115*, 2381–2388.
[5] G. H. Smith, *Development* **2005**, *132*, 681–687.
[6] V. Shinin, B. Gayraud-Morel, D. Gomes, S. Tajbakhsh, *Nat. Cell Biol.* **2006**, *8*, 677–687.
[7] P. Karpowicz, C. Morshead, A. Kam, E. Jervis, J. Ramunas, V. Cheng, D. van der Kooy, *J. Cell Biol.* **2005**, *170*, 721–732.
[8] M. J. Kiel, S. He, R. Ashkenazi, S. N. Gentry, M. Teta, J. A. Kushner, T. L. Jackson, S. J. Morrison, *Nature* **2007**, *449*, 238–242.
[9] M. L. Steinhauser, A. P. Bailey, S. E. Senyo, C. Guillermier, T. S. Perlstein, A. P. Gould, R. T. Lee, C. P. Lechene, *Nature* **2012**, *481*, 516–519.
[10] a) R. Castaing, G. Slodzian, *J. Microsc.* **1962**, *1*, 395–410; b) J. L. Guerquin-Kern, F. Hillion, J. C. Madelmont, P. Labarre, J. Papon, A. Croisy, *Biomed. Eng.* **2004**, *3*, 10; c) A. Gojon, N. Grignon, P. Tillard, P. Massiot, F. Lefebvre, M. Thellier, C. Ripoll, *Cell. Mol. Biol.* **1996**, *42*, 351–360; d) E. Hindie, B. Coulomb, R. Beaupain, P. Galle, *Biol. Cell* **1992**, *74*, 81–88.
[11] R. Peteranderl, C. Lechene, *J. Am. Soc. Mass Spectrom.* **2004**, *15*, 478–485.
[12] a) J. L. Guerquin-Kern, T. D. Wu, C. Quintana, A. Croisy, *Biochim. Biophys. Acta Gen. Subj.* **2005**, *1724*, 228–238; b) P. Hallegot, R. Peteranderl, C. Lechene, *J. Invest. Dermatol.* **2004**, *122*, 381–386; c) G. McMahon, H. F. Saint-Cyr, C. Lechene, C. J. Unkefer, *J. Am. Soc. Mass Spectrom.* **2006**, *17*, 1181–1187; d) C. P. Lechene, Y. Luyten, G. McMahon, D. L. Distel, *Science* **2007**, *317*, 1563–1566; e) M. R. Kilburn, D. L. Jones, P. L. Clode, J. B. Cliff, E. A. Stockdale, A. M. Herrmann, D. V. Murphy, *Plant Signaling Behav.* **2010**, *5*, 760–762.
[13] T. Li, T. D. Wu, L. Mazeas, L. Toffin, J. L. Guerquin-Kern, G. Leblon, T. Bouchez, *Environ. Microbiol.* **2008**, *10*, 580–588.
[14] M. L. Kraft, P. K. Weber, M. L. Longo, I. D. Hutcheon, S. G. Boxer, *Science* **2006**, *313*, 1948–1951.
[15] C. A. Bourgeois, R. Dennebouy, A. Gibaud, M. Gerbault-Seureau, B. Malfoy, G. Slodzian, P. Galle, B. Dutrillaux, *Chromosome Res.* **1996**, *4*, 574–582.
[16] A. Cabin-Flaman, A. F. Monnier, Y. Coffinier, J.-N. Audinot, D. Gibouin, T. Wirtz, R. Boukherroub, H.-N. Migeon, A. Bensimon, L. Jannière, C. Ripoll, V. Norris, *Anal. Chem.* **2011**, *83*, 6940–6947.
[17] D.-S. Zhang, V. Piazza, B. J. Perrin, A. K. Rzadzinska, J. C. Poczatek, M. Wang, H. M. Prosser, J. M. Ervasti, D. P. Corey, C. P. Lechene, *Nature* **2012**, *481*, 520–524.
[18] G. Legent, A. Delaune, V. Norris, A. Delcorte, D. Gibouin, F. Lefebvre, G. Misevic, M. Thellier, C. Ripoll, *J. Phys. Chem. B* **2008**, *112*, 5534–5546.

Received: March 29, 2012
Published online on ■■ ■■, 0000



  

**MIMS visualises metabolism:** A recent publication by Steinhauser and co-workers presents a novel application of multi-isotope mass spectrometry (MIMS) to visualise physiological metabolism in live mammalian organisms, and validate the 'immortal strand hypothesis' of asymmetric chromosomal division of stem cells in the small intestine.

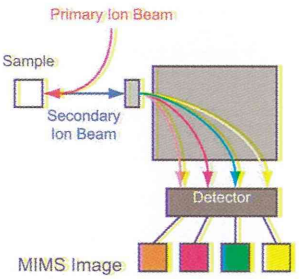


*K. Goto, M. Waki, T. Takahashi, M. Kadowaki, M. Setou**

■■ – ■■

**High-Resolution Multi-isotope Imaging Mass Spectrometry Enables Visualisation of Stem Cell Division and Metabolism**

Biochimica et Biophysica Acta xxx (2011) xxx–xxx

Contents lists available at ScienceDirect

Biochimica et Biophysica Acta

journal homepage: www.elsevier.com/locate/bbalip

Review

# Imaging mass spectrometry for lipidomics☆

Naoko Goto-Inoue [a], Takahiro Hayasaka [a], Nobuhiro Zaima [b], Mitsutoshi Setou [a,*]

[a] Department of Molecular Anatomy, Molecular Imaging Frontier Research Center, Hamamatsu University School of Medicine, 1-20-1 Handayama, Higashi-ku, Hamamatsu, Shizuoka 431-3192, Japan

[b] Department of Applied Biological Chemistry, Graduate School of Agriculture, Kinki University, Japan

ARTICLE INFO

*Article history:*
Received 14 December 2010
Received in revised form 15 March 2011
Accepted 16 March 2011
Available online xxxx

*Keywords:*
Lipidomics
Imaging mass spectrometry
Matrix-assisted laser desorption/ionization

ABSTRACT

Matrix-assisted laser desorption/ionization mass spectrometry (MALDI-MS) is a powerful tool that enables the simultaneous detection and identification of biomolecules in analytes. MALDI-imaging mass spectrometry (MALDI-IMS) is a two-dimensional MALDI-MS technique used to visualize the spatial distribution of biomolecules without extraction, purification, separation, or labeling of biological samples. This technique can reveal the distribution of hundreds of ion signals in a single measurement and also helps in understanding the cellular profile of the biological system. MALDI-IMS has already revealed the characteristic distribution of several kinds of lipids in various tissues. The versatility of MALDI-IMS has opened a new frontier in several fields, especially in lipidomics. In this review, we describe the methodology and applications of MALDI-IMS to biological samples. This article is part of a Special Issue entitled: Lipodomics and Imaging Mass Spectrometry.



## 1. Introduction

Lipids comprise a wide range of molecules such as fatty acids, glycerolipids, glycerophospholipids, sphingolipids, etc. These lipids have a wide range of biological functions, and each cell type exhibits a different lipid composition and distribution. For comprehensive lipid analyses, we use a "lipidomics" approach, which provides further insights into complex metabolic networks of biological systems. Mainly, lipidomics approaches have been demonstrated by the use of mass spectrometry (MS) to perform full characterization of lipid molecular species [1–4]. Qualitative and quantitative knowledge of the lipid composition is the first step for lipidomics. The most widely used MS instrument is MS coupled with liquid chromatography (LC)–electrospray ionization (ESI) [4]. LC–ESI–MS can quantify the amounts of lipids as well as identify the structure of lipid molecules. Many reports have shown that shot-gun lipidomics analyses are the most suitable analytical method to investigate the full range of lipid molecules in cells or tissues or to find molecular-level indications of diseases by comparing the distribution of various lipid molecules in diseased tissue with that in control samples [5,6]. However, this technique entails extraction and purification steps, leading to the loss of the lipid distribution over the biological tissue. Meanwhile, numerous techniques of chemical imaging enable the detection and the localization of lipids. Staining with Nile Red, Oil Red O [7], osmium tetroxide [8], or BODIPY is a common method to localize the lipid fraction on frozen sections, whereas few specific lipid antibodies [9] are commercially available. These approaches target either the complete lipid fraction or only one specific family, not molecular species with a wide variety of fatty acid compositions. By contrast, imaging mass spectrometry (IMS) is a relatively new imaging method based on MS. IMS is a two-dimensional MS technique used to visualize the spatial distribution of biomolecules. Several ionization methods, including secondary ion mass spectrometry (SIMS), desorption electrospray ionization (DESI), laser ablation electrospray ionization (LAESI), nanostructure-initiator (NI), and matrix-assisted laser desorption/ionization (MALDI), have been investigated as methods of IMS. In this review, we focus on lipid imaging by MALDI-MS because MALDI-IMS is the most common IMS method for lipid imaging. Indeed, the versatility of MALDI-IMS has opened a new frontier in several other fields, as well as lipidomics.

## 2. Instruments for IMS

IMS is a remarkable technology that enables us to determine the distribution of biological molecules present in tissue sections by direct ionization and detection. This technique is now widely used for in situ imaging of endogenous or exogenous molecules. There are several kinds of instruments used for IMS.

### 2.1. Ionization methods for IMS

IMS techniques include various ionization methods that can ionize the analytes on the surface, such as SIMS [10–13], DESI [14–18], LAESI [19,20], NI [21,22], and MALDI [23–25]. These ionization methods have both merits and demerits; therefore, users have to consider carefully which method is best for their analyses.

☆ This article is part of a Special Issue entitled: Lipodomics and Imaging Mass Spectrometry.

* Corresponding author. Tel./fax: +81 53 435 2292.
*E-mail address:* setou@hama-med.ac.jp (M. Setou).

1388-1981/$ – see front matter © 2011 Elsevier B.V. All rights reserved.
doi:10.1016/j.bbalip.2011.03.004